

Stress Transfer Efficiency in Semicrystalline-Based Composites Comprising Transcrystalline Interlayers

A. Gati and H. D. Wagner*

Department of Materials and Interfaces, The Weizmann Institute of Science, Rehovot 76100, Israel

Received July 12, 1996

Revised Manuscript Received April 3, 1997

The strength of the interface, under shearing forces, reflects the ability of composites to transfer stresses from externally applied forces, via the matrix, to the fiber. The parameters commonly used to characterize this ability are the interfacial shear strength (ISS), τ_{ic} ,^{1,2} or the interfacial strain energy release rate, G_i .^{3,4} A number of micromechanical tests, such as the fragmentation test,^{4,5} the microbond test,^{6,7} the microindentation test,⁸ and the pull-out test,^{9,10} have been used over the last few years to determine τ_{ic} and G_i .

A number of physical and chemical parameters may influence the stress transfer ability of the interface. One of these is the matrix morphology around the reinforcing fibers. Indeed, a fiber in a semicrystalline polymer melt may act as a preferred nucleating site for the growth of crystalline spherulites. Provided there is a high density of nucleating sites along the fiber surface¹¹ and specific thermal conditions are met, the resulting spherulitic growth will be restricted in the lateral direction, normal to the fiber surface, so that a columnar layer, known as transcrystallinity,¹² will develop and enclose the fiber.^{13,14}

Transcrystallinity might possibly have an important effect on the thermomechanical properties of the composites. For example, theoretical calculations¹⁵ predict strong effects regarding thermal residual stresses resulting from specimen preparation, due to the extensive anisotropy of the transcrystalline microstructure. This has not yet been experimentally demonstrated. As to the effect of transcrystallinity on the interfacial mechanical properties, the phenomenon is not yet fully understood and the literature data published so far is somewhat ambiguous. A few examples will show this. Using polypropylene as a matrix, Folkes and Wong¹⁶ concluded that transcrystalline morphology induced around glass fibers causes a reduction in the ISS. Klein and Marom¹⁷ arrived at a similar conclusion using HM carbon/Nylon-66. An opposing view was obtained by Incardona et al.¹⁸ using HM carbon/J-polymer and, more recently, by Wood and Marom¹⁹ using HM carbon/polycarbonate. On the other hand, Hsiao and Chen²⁰ claimed that transcrystallinity has apparently no effect on the ISS of various composite systems. However, later²¹ these authors claimed that transcrystallinity improved the fiber/matrix adhesion.

The influence of transcrystallinity on the stress transfer ability in poly(caprolactone) (PCL)/Kevlar 149 model microcomposites is investigated here by means of the microbond pull-out test. We present a reliably large set of data collected with almost fully transcrystalline and quasi-amorphous droplets, respectively, in an attempt to provide a more definitive answer to the

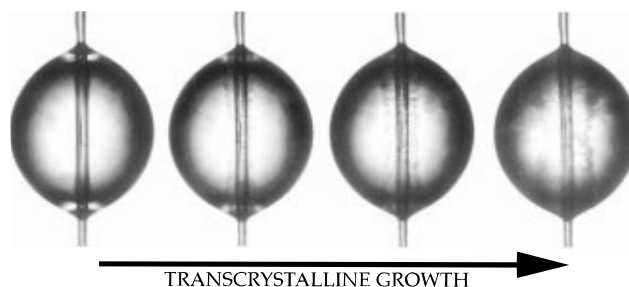


Figure 1. Nucleation and growth of a PCL transcrystalline layer from the surface of a single Kevlar 149 fiber (diameter: 12.5 μm), as viewed by optical microscopy. The liquid droplet is first held at 85 $^{\circ}\text{C}$ and subsequently cooled down to a 50 $^{\circ}\text{C}$ isotherm (where the pictures were taken), followed by fast quenching.

question of the effect of transcrystallinity on interfacial adhesion and fiber/matrix stress transfer.

Single filaments of Kevlar 149 fibers (E. I. du Pont de Nemours, Inc.), with a nominal diameter of 12.5 μm , were carefully extracted from a fiber bundle and stretched horizontally across spacers, resting on a glass slide, using 0.25 g weights attached to the ends of each filament. Poxipol epoxy cement was used to fasten the filaments to the spacers, and the glass slide was then inserted into a Mettler FP90 hot stage at 85 $^{\circ}\text{C}$. A small amount of poly(caprolactone) (Polysciences, Catalog No. 7039) was subsequently melted (melting point $T_m = 60$ $^{\circ}\text{C}$) on the glass slide, next to the fiber, and droplets of molten PCL were carefully spread on each filament using the tip of a scalpel. The samples were kept at 85 $^{\circ}\text{C}$ for 10 min before being cooled to a 50 $^{\circ}\text{C}$ isotherm at a rate of 20 $^{\circ}\text{C min}^{-1}$.

One set of samples was left at this temperature for 1 h, which was sufficient for an almost fully transcrystalline droplet to develop (Figure 1), before being quenched using cold nitrogen gas. On the other hand, another set of samples was immediately quenched by the cold gas which resulted in a quasi-amorphous droplet, that is, a droplet with a very finely dispersed spherulitic microstructure that has an amorphous appearance under the microscope. The nitrogen gas was cooled by burying the 2 m long coil that carried the gas from the reservoir, in dry ice. The gas temperature, measured with a thermocouple immediately after opening the reservoir valve, was -30 $^{\circ}\text{C}$. Quenching times were on the order of a few seconds, and the gas reservoir valve was opened at intervals of no less than 30 min, to allow the gas to cool down. After quenching, the droplet length and thickness, and the fiber diameter, were measured by optical microscopy. While still on the frame, a fiber was placed between two pairs of rectangular aluminum tabs, with a pair at each side of the droplet, and the tabs were fastened together (Loctite, Super Glue 3) such that at least a 10 mm distance was left between the tabs and the droplet. The fiber was subsequently cut away from the frame, and a 0.25 g weight was fastened to one set of tabs, to ensure that the fiber remained under slight tension during the microbond experiment, while the other set of tabs was inserted within the upper jaws of the tensile testing apparatus. All microbond tests were conducted in a tensile testing machine (Instron Ltd., Model 4502) at a strain rate of 60 $\mu\text{m min}^{-1}$. The tips of a Vernier caliper were placed above the droplet, close to the fiber, such that when these were lowered, a shearing force was exerted on the droplet. At a critical value of this force,

* Author to whom correspondence is addressed. Telephone: (972) 8 934 2594. Fax: (972) 8 934 4137. Email: cpwagner@wis.weizmann.ac.il.

debonding of the interface between the fiber and the matrix occurred, along the whole length of the droplet. Beyond that point, a constant residual fiber–droplet friction stress was observed. A large number of droplet/fiber specimens (approximately 50) were tested for both sets (amorphous and transcrystalline). Due to imperfect fiber alignment during pullout, or machine noise, or droplet imperfections, only 37 samples, for each set, yielded successful test results.

For the purpose of optical microscope observation, some of the specimens were then handled as follows. The fiber was hung vertically, along the central axis of a plastic mold which was subsequently filled with epoxy (Bisphenol A derivate, DER 331, and pentaethylene tetramine hardener, DEH 26, from Dow Chemical International) and allowed to cure for 24 h at room temperature. A disk was then cut out from the hardened epoxy cylinder, and one face was polished and microtomed in successive steps until about halfway into the droplet. The differences in morphology between the transcrystalline and amorphous droplets could then easily be observed under the microscope (Figure 2).

Two approaches were followed to analyze the microtomed test data, namely, a simple classical strength-of-materials approach and Nairn's recently developed variational mechanics analysis.^{22,23} The former assumes a uniform stress state in the droplet during shearing. This is a weak assumption but is nevertheless used here because this approach is still widely applied. The latter is a more exact analysis provided by Nairn^{3,22,23} and the key parameter is an energy-based one.

To calculate the interfacial shear strength, we assumed that the droplet shears off the fiber when the average shear stress at the interface, τ , reaches the ISS, τ_{ic} , i.e., when the experimentally observable applied force becomes large enough to rupture the interface.^{1,2} Thus,

$$F_d = 2\pi r_f l \tau_{ic} \quad (1)$$

where r_f is the fiber radius, l is the embedded fiber length, and F_d is the applied load at debonding.

The energy release rate for initiation of an interfacial crack, G_i , was calculated by assuming that specimen failure occurs when G_i reaches the critical energy release rate for the interface or the interfacial toughness, G_{ic} . Prediction of debonding is based on the energy release rate for initiation of an interfacial crack at the point where the droplet is contacted by the Vernier caliper tips. This is a logical assumption since this is the point where the interfacial stresses are the highest.³ The relationship between the applied load at specimen failure, F_d , and the total strain energy release rate, G_{ic} , is

$$F_d = \pi r_f^2 \left\{ -\frac{D_{3s}\Delta T}{C_{33s}} + \sqrt{\frac{2G_{ic}}{r_f C_{33s}}} \right\} \quad (2)$$

where r_f is the fiber radius, $\Delta T = T_{test} - T$, where T_{test} is the temperature during the microbond test and T is the stress-free temperature, and the constants, C_{33s} and D_{3s} , are given by

$$C_{33s} = \frac{1}{2} \left(\frac{1}{E_A} + \frac{V_f}{V_m E_m} \right) \quad (3)$$

$$D_{3s} = \frac{1}{2} (\alpha_A - \alpha_m) \quad (4)$$

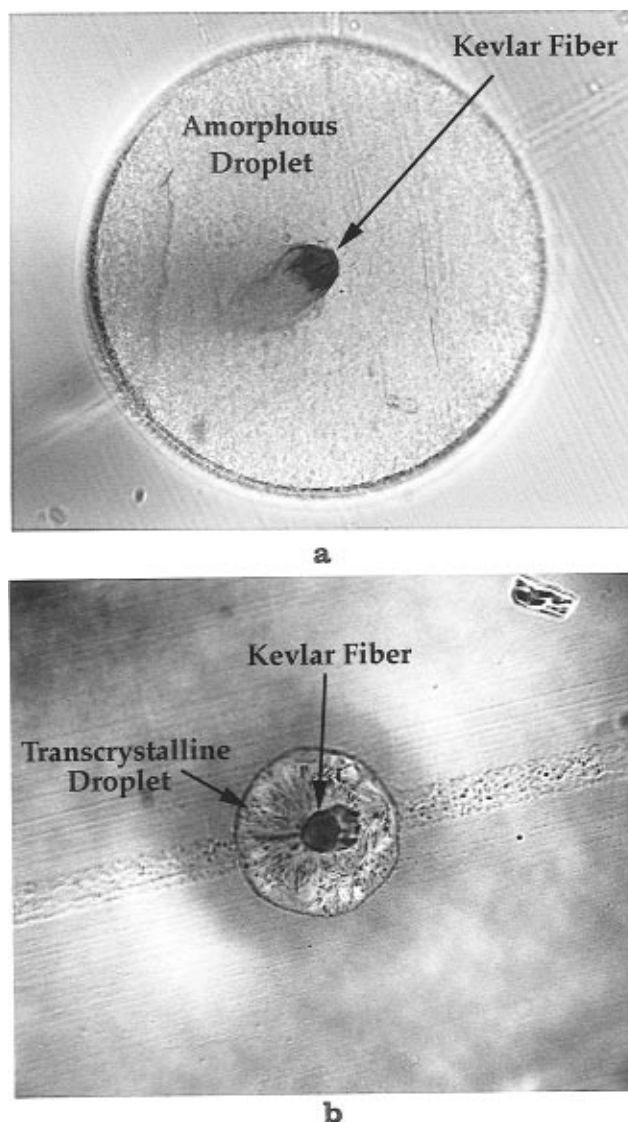


Figure 2. Optical micrograph of microtomed droplet cross sections for (a) quasi-amorphous and (b) transcrystalline droplet of PCL on the surface of a Kevlar 149 fiber. The smeared "tails" extending from the fiber section, as well as the transverse line in b, result from the cutting procedure. The quasi-amorphous droplet appears as a uniform cross section, whereas the transcrystalline droplet shows a distinct crystalline morphology.

where E is the Young's modulus, V is the volume fraction, α is the coefficient of thermal expansion, and subscripts f, m, and A denote fiber, matrix, and axial, respectively. The first term in parentheses in eq 2 results from the thermal stresses generated from droplet cooling. Note that even though the samples were quenched from 50 to -30 °C, as described earlier, we used $\Delta T = -25$ °C, since the microbond tests were carried out at room temperature.

The fiber–droplet debonding force, F_d , was plotted against embedded length (Figure 3), and a linear best fit of eq 1 was performed through the data points, from which τ_{ic} was obtained. Likewise, a nonlinear fit of eq 2 to the data points was used to calculate G_{ic} , by means of a Marquardt–Levenberg algorithm.²⁴ In addition, values of τ_{ic} and G_{ic} were calculated individually for each data point and averaged over the set (τ_{ic}^* and G_{ic}^*), by using eqs 1 and 2, respectively. The results are reported in Table 1. As seen, the values of τ_{ic} and G_{ic} are of the same order as those normally observed with other

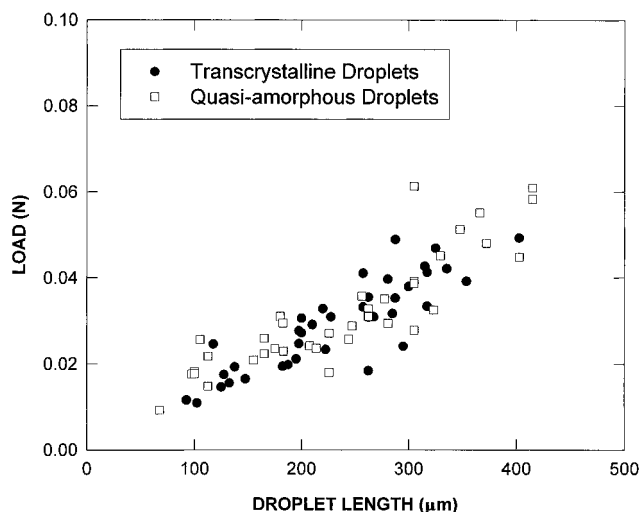


Figure 3. Applied load vs fiber embedded length plot for transcrystalline and quasi-amorphous droplets.

Table 1. Values of the ISS and Critical Energy Release Rate, as Measured by the Microbond Experiment, for Quasi-Amorphous and Transcrystalline Droplets of Poly(caprolactone)/Kevlar 149^a

	shear stress model		critical energy release model	
	τ_{ic} (MPa)	τ_{ic}^* (MPa)	G_{ic} (J m ⁻²)	G_{ic}^* (J m ⁻²)
quasi-amorphous	3.04 ($r^2 = 0.75$)	3.54 ± 0.84	6.56	6.97 ± 3.05
transcrystalline	3.01 ($r^2 = 0.75$)	3.23 ± 0.61	5.83	5.70 ± 1.89

^a τ_{ic} and G_{ic} are obtained by fitting eqs 1 and 2 to the data points, whereas τ_{ic}^* and G_{ic}^* are the average of the individually calculated values for each droplet. The temperature decrement is $\Delta T = -25$ °C.

thermoplastic-based composites. Moreover, there is no statistically significant difference between the two data sets. The Student's *t* test for the equal mean hypothesis ($\mu_{transcrystalline} - \mu_{amorphous} = 0$) can only be rejected for G_{ic}^* at the 5% significance level but holds for G_{ic}^* at the 1% significance level and for τ_{ic}^* at the 5% and 1% significance levels. Thus, with the fiber-matrix composite system studied here, transcrystals are most certainly neither beneficial nor detrimental to the fiber-matrix stress transfer ability. This conclusion, which is based on results from a reliably large sample of specimens, contradicts several of the previously published results but confirms the assertion of Hsiao and Chen in their earlier work.²⁰

Finally, SEM observations did not reveal significant differences between the fracture surfaces of the fibers for the transcrystalline interphase and fully amorphous matrix cases. We conclude that, in both cases, there is

a high probability that the failure locus is at the aramid/polypropylene interface.

In summary, PCL exhibits transcrystalline nucleation and growth from the surface of a Kevlar 149 fiber substrate, when a droplet of the polymer is melted and supercooled on the fiber. Large data sets were produced to measure the adhesion characteristics of both transcrystalline and amorphous droplets on a fiber, using the microbond experiment. The results clearly indicate that the presence of transcrystallinity produces little if any effect on the stress transfer ability of the interface between PCL and Kevlar 149.

Acknowledgment. We thank the MINERVA Foundation, Munich, Germany, for supporting this research.

References and Notes

- (1) Kelly, A.; Tyson, W. R. *J. Mech. Phys. Solids* **1965**, *13*, 329.
- (2) Cox, H. L. *Br. J. Appl. Phys.* **1952**, *3*, 72.
- (3) Nairn, J. A.; Scheer, R. J. *J. Adhes.* **1995**, *53*, 45.
- (4) Wagner, H. D.; Nairn, J. A.; Detassis, M. *Appl. Compos. Mater.* **1995**, *2*, 107.
- (5) Wagner, H. D.; Eitan, A. *Appl. Phys. Lett.* **1990**, *56*, 1965.
- (6) Wagner, H. D.; Gallis, H. E.; Wiesel, E. *J. Mater. Sci.* **1993**, *28*, 2238.
- (7) Rolel, D.; Yavin, E.; Wachtel, E.; Wagner, H. D. *Compos. Interfaces* **1993**, *1*, 225.
- (8) Desaegeer, M.; Verpoest, I. *Compos. Sci. Technol.* **1993**, *48*, 215.
- (9) Chua, P. S.; Piggott, M. R. *Compos. Sci. Technol.* **1985**, *22*, 33.
- (10) Meretz, S.; Auersch, W.; Marotzke, C.; Schulz, E.; Hampe, A. *Compos. Sci. Technol.* **1993**, *48*, 285.
- (11) Hoecker, F.; Karger-Kocsis, J. *Polym. Bull.* **1993**, *31*, 707.
- (12) Keller, A. *J. Polym. Sci.* **1955**, *15*, 31.
- (13) Folkes, M. J.; Hardwick, S. T. *J. Mater. Sci. Lett.* **1987**, *6*, 656.
- (14) Hsiao, B. S.; Chen, E. J. H. *Mater. Res. Soc. Symp. Proc.* **1990**, *170*, 117.
- (15) Wagner, H. D. *Phys. Rev. B* **1996**, *53*(9), 5055.
- (16) Folkes, M. J.; Wong, W. K. *Polymer* **1987**, *28*, 1309.
- (17) Klein, N.; Marom, G. Private Communication, The Hebrew University of Jerusalem, 1994.
- (18) Incardona, S.; Migliaresi, C.; Wagner, H. D.; Gilbert, A. H.; Marom, G. *Compos. Sci. Technol.* **1993**, *47*, 43.
- (19) Wood, J. R.; Wagner, H. D.; Marom, G. *J. Mater. Sci. Lett.* **1995**, in press.
- (20) Hsiao, B. S.; Chen, E. J. H. *Mater. Res. Soc. Symp. Proc.* **1990**, *170*, 117.
- (21) Hsiao, B. S.; Chen, E. J. H. In *Controlled Interphases in Composite Materials. Proceedings of the Third International Conference on Composite Interfaces (ICCI-3)*, May 21–24, 1990, Cleveland, OH, Elsevier Science Publishing: New York, 1990; pp 613–622.
- (22) Nairn, J. A. *Mech. Mater.* **1992**, *13*, 131.
- (23) Nairn, J. A.; Scheer, R. J. *Compos. Eng.* **1992**, *2* (No. 8), 641.
- (24) Press, W. H.; Flannery, B. P.; Teukolsky, S. A.; Vetterling, W. T. *Numerical Recipes*; Cambridge University Press: Cambridge, 1986.

MA961027Z